scientific reports

Check for updates

OPEN

Mesenchymal stem cells modulate breast cancer progression through their secretome by downregulating ten-eleven translocation 1

Romina Motamed[1,3], Keyvan Jabbari[1,3], Mahboubeh Sheikhbahaei[1], Mohammad H. Ghazimoradi[1], Sara Ghodsi[1], Motahareh Jahangir[1], Neda Habibi[2] & Sadegh Babashah[1]✉

Mesenchymal stem cells (MSCs) have emerged as crucial players within the tumor microenvironment (TME), contributing through their paracrine secretome. Depending on the context, the MSC-derived secretome can either support or inhibit tumor growth. This study investigates the role of MSC-derived secretome in modulating breast cancer (BC) cell behavior, with a focus on ten-eleven translocation 1 (TET1), a DNA demethylase with known oncogenic properties in triple-negative breast cancer (TNBC). We first isolated and characterized human bone marrow-derived MSCs, and then assessed the impact of their secretome on BC cells. Treatment with the MSC-derived secretome significantly inhibited the proliferation and migration of both MDA-MB-231 and MCF-7 BC cell lines, resulting in reduced cell viability and migration rates compared to control cells. Western blot analyses revealed downregulation of Cyclin D1 and c-Myc, along with decreased expression of N-cadherin and increased expression of E-cadherin, indicating potential inhibition of the epithelial-to-mesenchymal transition. Differential gene expression analyses highlighted TET1 as significantly upregulated in TNBC tissues compared to normal samples. Further experiments confirmed that the MSC-derived secretome downregulated TET1 expression in BC cells, as evidenced by RT-qPCR and western blot analyses. To explore TET1's functional role, we silenced TET1 with siRNAs, observing cell cycle arrest and enhanced apoptosis—effects that mirrored those seen with MSC-secretome treatment. Notably, TET1 knockdown also increased MDA-MB-231 cell sensitivity to cisplatin, suggesting a role for TET1 in chemoresistance. These findings provide insight into the ability of MSCs to modulate BC cell progression through their secretome, highlighting the involvement of TET1 downregulation in inhibiting BC cell progression and enhancing cisplatin chemosensitivity. The MSC-derived secretome thus holds promise as an innovative, cell-free therapeutic approach in BC treatment.

Keywords Mesenchymal stem cells, Secretome, Breast cancer, TET1

Understanding the role of the unique tumor microenvironment (TME) in the progression of triple-negative breast cancer (TNBC) is a complex process. This complexity arises from the dynamic and ever-changing nature of the microenvironment, which comprises various components, including fibroblasts, immune-suppressive cells, and soluble factors[1–4]. The rapid proliferation of tumor cells in TNBC results in hypoxia, which in turn leads to the reprogramming of tumor cells within the TME[5]. Tumor cells and the TME continuously adapt to changing conditions, and the dynamic interactions between them significantly influence tumor development and growth. A substantial body of research has demonstrated that different molecular subtypes of TNBC, the most common form of invasive breast cancer, exhibit distinct TME patterns[6]. While alterations in genetic material are the primary drivers of BC development, the TME plays a crucial role in its progression[7].

Mesenchymal stem cells (MSCs) represent a burgeoning area of research focused on their role in maintaining tissue homeostasis and regenerating damaged tissues[8–10]. MSCs are increasingly recognized for their dual and complex role in cancer, possessing the potential to both inhibit and promote tumor progression. In response

[1]Department of Molecular Genetics, Faculty of Biological Sciences, Tarbiat Modares University, P.O. Box: 14115-154, Tehran, Iran. [2]Department of Biomedical Engineering, University of North Texas, Denton, TX, USA. [3]Romina Motamed and Keyvan Jabbari contributed equally to this work. ✉email: babashah@modares.ac.ir

to their microenvironment, MSCs exhibit a robust paracrine effect, driven by the abundance of bioactive molecules[11]. In the context of TNBC, various components of the TME may be influenced by MSCs through direct cell interactions or the release of cytokines, chemokines, growth factors, and extracellular vesicles (EVs)[12,13]. A study demonstrated that intravenous administration of MSCs significantly reduces tumor growth in BC cells compared to the control group[14]. The secretome, which encompasses a diverse array of molecules secreted by MSCs, can influence gene expression and cellular communication[15]. The MSC-derived secretome contributes to various physiological processes through paracrine mechanisms, holding promise as a therapeutic option for various diseases[16]. Additionally, the MSC-derived secretome has shown significant advantages as a cell-free therapy in regenerative medicine[17].

Characterized by significant heterogeneity and molecular diversity, TNBC poses a substantial risk of relapse and metastasis. TNBCs also exhibit distinct DNA methylation profiles, making them the most hypomethylated among BC subtypes, including ER-positive and PR-positive tumors[18,19]. DNA methylation plays a pivotal role in BC, and the modulation of this process is regulated by a balance between DNA methyltransferases (DNMTs) and DNA demethylases, such as ten-eleven translocation1 (TET1)[20]. TET enzymes catalyze the oxidation of the 5-methyl group of cytosine, leading to intermediate derivatives such as 5-hydroxymethylcytosine (5-hmC) and, subsequently, more oxidized products. This enzymatic process effectively reverses DNA methylation[21]. Among the TET family, TET1 stands out as a particularly notable member, exhibiting dual roles as either a promoter of cancer development or a suppressor of tumor growth during tumorigenesis[22].

This study aimed to investigate the potential paracrine effects of MSCs on the progression of BC cells. We sought to evaluate whether the secretome of stromal cells influences the reduction of the malignant phenotype and progression of BC cells. Additionally, we assessed the impact of MSC secretions on TET1 expression and their role in modulating breast cancer's response to cisplatin treatment. Overall, our findings may provide valuable insights into how MSC secretions affect tumor cell behavior and illuminate the role of demethylase enzyme expression in the progression of BC.

Results

Isolation and characterization of bone marrow mesenchymal stromal cells

According to the criteria set by the International Society for Cellular Therapy (ISCT), the characterization of human bone marrow mesenchymal stromal cells (BM-MSCs) requires a detailed evaluation of specific cell surface markers and functional properties. The ISCT guidelines specify that MSCs must express markers such as CD90 and CD105, while lacking expression of hematopoietic markers like CD34. Flow cytometry analysis of cell surface markers demonstrated positive expression of CD73, CD90, and CD105, with no expression of hematopoietic cell lineage markers CD34 and CD11b (Fig. 1A). Additionally, in vitro differentiation assays confirmed efficient osteogenic and adipogenic differentiation (Fig. 1B), validating the multipotency of the isolated BM-MSCs.

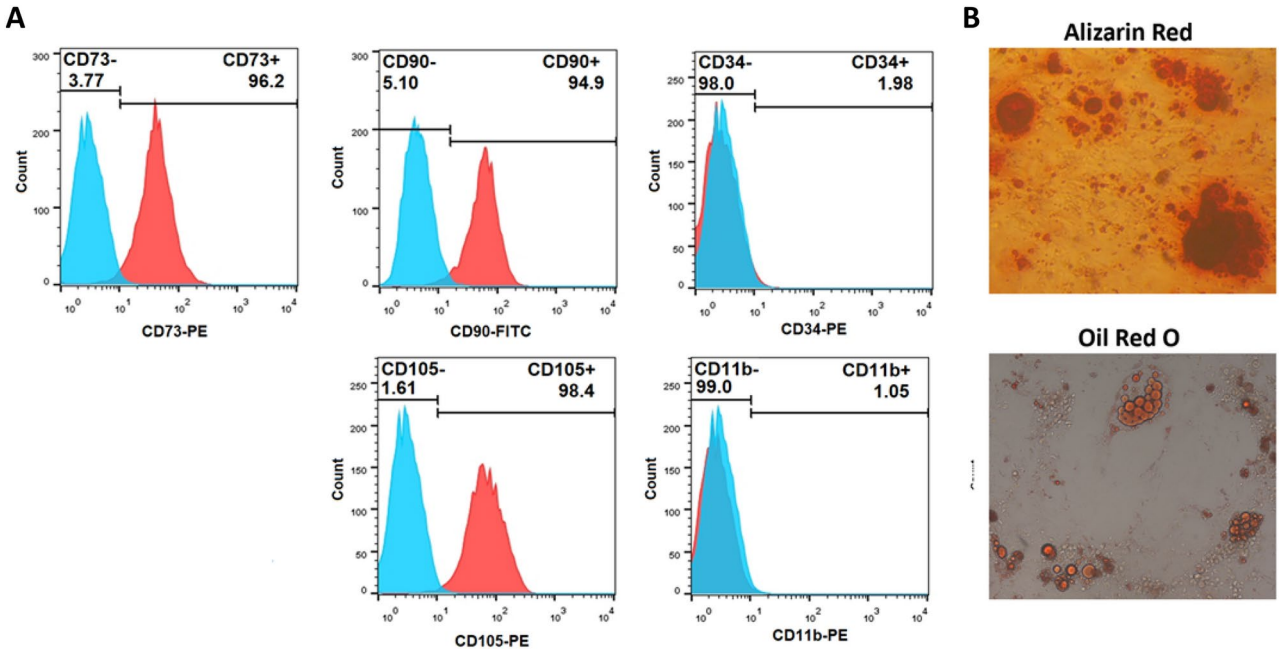

Fig. 1. Characterization of human bone marrow-derived mesenchymal stem cells (BM-MSCs). **(A)** Flow cytometry histograms showing that isolated BM-MSCs were positive for surface markers CD73 (96.2%), CD90 (94.9%), CD105 (98.4%), but negative for CD34 (1.98%) and CD11b (1.05%). (**B**) The multipotent differentiation potential of BM-MSCs was confirmed through Alizarin Red staining for osteogenic differentiation and Oil Red O staining for adipogenic differentiation.

MSC-derived secretome inhibits breast cancer progression in vitro

To evaluate the paracrine effects of MSCs on the tumor microenvironment of cancer cells, the impact of MSC-derived secretome (MSC-secretome) on the behavior of breast cancer cells was investigated. Treatment of MDA-MB-231 BC cells with MSC-secretome led to a reduction in cell proliferation. The results clearly demonstrated the inhibitory effect of MSC-secretome on the proliferation of MDA-MB-231 cells (Fig. 2A, B). To investigate whether MSC-secretome affects BC cell migration, MDA-MB-231 cells were incubated with either MSC-derived secretome or PBS. A scratch wound healing assay was performed to analyze the cell-covered areas and measure the distances migrated by cells at 0, 24 h, and 48 h after wounding. Results indicated that MSC-secretome significantly reduced the migration rate of MDA-MB-231 cells (Fig. 2C, D). Similar results were obtained when this experiment was repeated in another breast cancer-derived cell line, MCF-7 (Fig. 2E, F). Overall, these

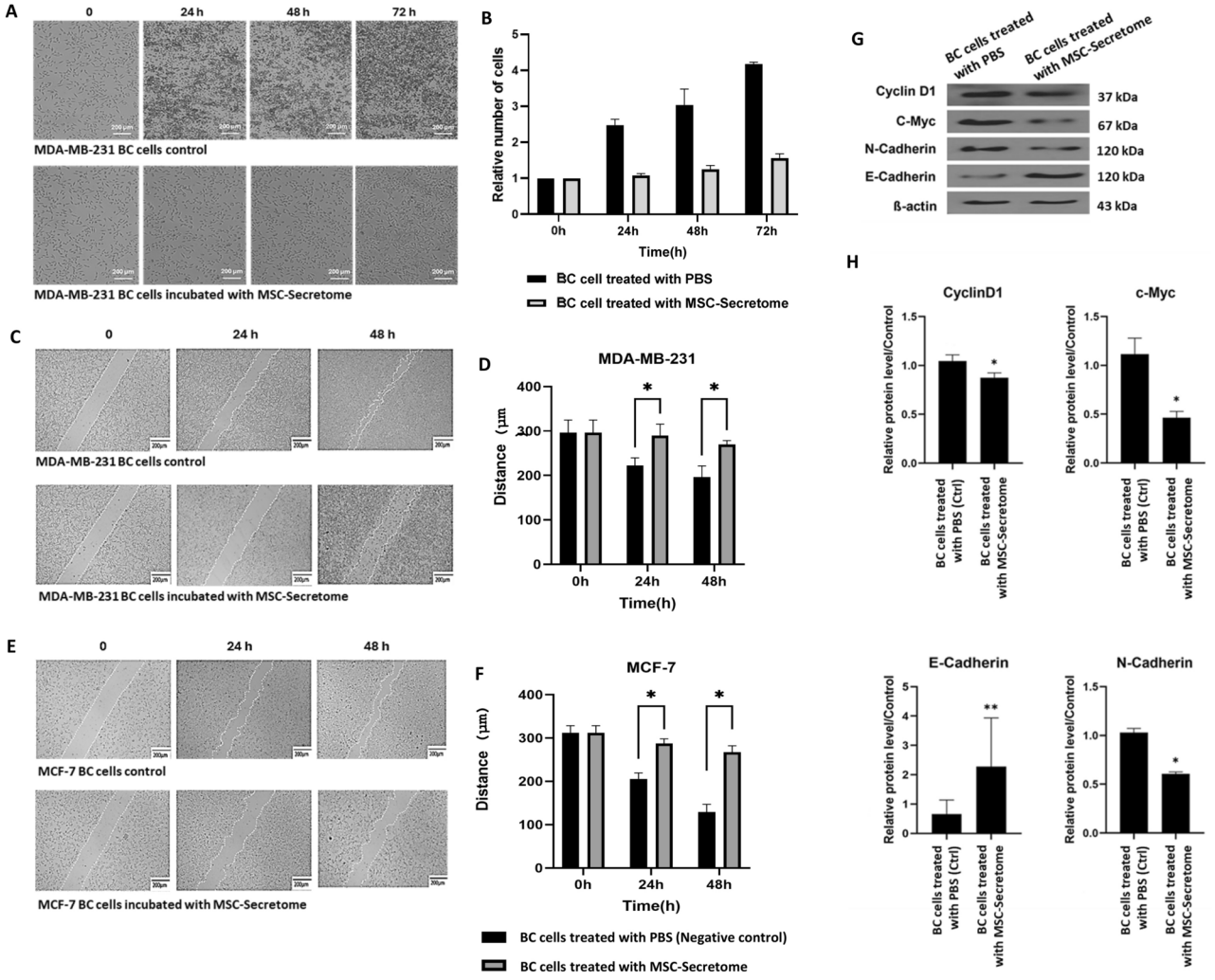

Fig. 2. MSC-derived secretome inhibits BC cell progression. (**A**) Representative images showing proliferation and morphological changes in MDA-MB-231 BC cells following treatment with MSC-derived secretome compared to control conditions at various time points. (**B**) Proliferation of MDA-MB-231 cells was measured after treatment with MSC-derived secretome, which exhibited an inhibitory effect on the relative number of MDA-MB-231 breast cancer cells. This inhibition was observed at four time points: 0, 24, 48, and 72 h post-treatment. (**C–F**) Representative images of MDA-MB-231 **(C)** and MCF-7 **(E)** BC cells cultured with MSC-derived secretome or control medium containing PBS, at 24 and 48 h post-scratch wounding. Magnification: 10×, Scale bar = 200 µm. Quantitative analysis of cell migration revealed significantly reduced migration potential in MDA-MB-231 **(D)** and MCF-7 **(F)** cells treated with MSC-derived secretome compared to those cultured in control medium with PBS. (**G, H**) Western blot analysis demonstrated downregulation of Cyclin D1, c-Myc, and the EMT marker N-cadherin, along with up-regulation of the epithelial marker E-cadherin in MDA-MB-231 BC cells 48 h after MSC-secretome treatment, compared to the corresponding control cells. β-actin was used as a loading control. Western blot images represent at least three independent experiments **(G).** Original blots are presented in Supplementary Fig. 1. Band densities were quantified using ImageJ software and presented as relative intensities **(H)**. Data are expressed as the mean ± SD from three independent experiments; **P*-value < 0.05, ***P*-value < 0.01.

findings demonstrated that the migration of both MDA-MB-231 and MCF-7 BC cells into the scratched areas was slower in the presence of MSC-derived secretome compared to the control group.

Inhibitory effects of MSC-derived secretome on BC cell progression through modulation of EMT markers

Cyclin D1 plays a critical role in facilitating the transition from the G1 to the S phase of the cell cycle, making it a key protein associated with tumor progression. Additionally, c-Myc, a proto-oncogene, regulates the G1/S checkpoint by promoting the upregulation of cyclin D[23]. E-cadherin and N-cadherin are crucial for their roles in cellular adhesion and involvement in the epithelial-to-mesenchymal transition (EMT). Their inverse expression patterns provide valuable insights into the EMT process, which is vital for tumor progression and metastasis. To confirm the inhibitory effects of MSC-secretome on BC cell progression, the expression levels of cyclin D1 and c-Myc were measured. The western blot results demonstrated that MSC-secretome treatment significantly reduced the expression of both genes (Fig. 2G, H). Moreover, incubation with MSC-secretome led to an upregulation of E-cadherin expression and a significant reduction in N-cadherin expression (Fig. 2G, H). Overall, these findings suggest that the secretome released by MSCs may potentially slow the progression of BC cells by regulating proteins that play key roles in both cell cycle progression and EMT.

Differential expression analysis and identification of elevated TET1 expression in TNBC tumors: an RNA-Seq analysis

Global gene expression analysis was initially performed using the Gene Expression Omnibus (GEO) database, which enabled the comparison of expression profiles between control samples and triple-negative breast cancer (TNBC) tumors. Volcano plots were generated to visually represent the differential expression patterns, highlighting genes with statistically significant upregulation or downregulation. This analysis identified TET1 as one of the significantly differentially upregulated genes. Our results indicated that TET1 expression in TNBC tumors is significantly higher than in normal tissues, with a log fold change (log FC) of 1.4 in GSE58135 and 2.03 in GSE233242, both with a p-value < 0.05 (Fig. 3A, B).

MSC-derived secretome downregulates TET1 expression in breast cancer cells

Our bioinformatics analysis indicated that TET1 is significantly upregulated in TNBC (Fig. 3). Additionally, TET1 was found as a potential oncogene in TNBC[24]. Given that the tumor-suppressive role of MSC-secretome has been previously established, we aimed to investigate its effect on TET1 expression. To assess the role of TET1 in BC progression, we first evaluated TET1 gene expression in BC cell lines treated with MSC-secretome. RT-qPCR results showed that treatment with the MSC-derived secretome was associated with the downregulation of TET1 in BC cells (Fig. 3C). Meanwhile, to confirm that TET1 is indeed downregulated by MSC-secretome, western blot analysis was used to assess TET1 protein levels. A significant reduction in TET1 protein level was observed following MSC-secretome treatment on MDA-MB-231 BC cells (Fig. 3D, E). These findings indicate that MSC-derived secretome downregulates TET1 expression in breast cancer cells.

MSC-derived secretome and Tet-1 down-regulation induce cell cycle arrest in breast cancer cells

To further highlight the role of TET1 in BC progression, we examined the effect of TET1 suppression using specific siRNAs targeting TET1 (si-TET1). The results revealed similar outcomes and phenotypes comparable to those observed with MSC- secretome treatment, as detailed below. We transfected MDA-MB-231 cells with si-TET1 and found that siTET1 transfection resulted in a marked decrease in TET1 transcript expression (Fig. 4A). Subsequently, we examined the effects of MSC-derived secretome and si-TET1 treatments on cell cycle progression in MDA-MB-231 cells by analysing cell cycle distribution using flow cytometry. Compared to negative control cells, propidium iodide (PI) staining and flow cytometry revealed an increased cell population in the sub-G1 phase following treatment. The results indicated a higher proportion of cells in the sub-G1 phase in samples treated with either MSC-secretome or si-TET1 compared to the corresponding control cells (Fig. 4B). A similar result was observed with MSC-secretome treatment of MCF-7 cells. The increase in the sub-G1 cell population suggests that the cells are arrested in this phase and are prone to apoptosis following treatment (Fig. 4B).

Targeting TET1 promotes migration, triggers apoptosis, and enhances cisplatin sensitivity in breast cancer cells

To assess the contribution of TET1 suppression in the inhibitory effect of MSC-derived secretome on TNBC cell migration, we evaluated the impact of TET1 knockdown on the migration ability of MDA-MB-231 cells using a wound healing assay. The results showed that TET1 knockdown via si-TET1 treatment significantly reduced the migration ability of MDA-MB-231 cells at both 24- and 48-h time points compared to cells transfected with si-NC (Fig. 4C, D). Additionally, the findings revealed that TET1 knockdown enhanced apoptosis in MDA-MB-231 cells. The reduction in TET1 expression was significantly associated with an increase in apoptotic cell populations, as confirmed by flow cytometry analysis (Fig. 4E, F). Moreover, the sensitivity of MDA-MB-231 cells to cisplatin was assessed using the MTT assay, with cells exposed to various concentrations of cisplatin for 24 and 48 h to evaluate its cytotoxicity. Cisplatin exhibited a significant, dose- and time-dependent inhibition of MDA-MB-231 cell viability, as illustrated in Fig. 5A, B. Notably, the half-maximal inhibitory concentration (IC50) of cisplatin for MDA-MB-231 cells was 43.55 µM after 24 h, decreasing to 17.20 µM after 48 h (Fig. 5A, B). Using the 48-h IC50 value for siTET1-treated cells showed a more rapid decrease in cell viability, indicating that TET1 suppression with siTET1 sensitized MDA-MB-231 cells to cisplatin (Fig. 5C). These findings highlight

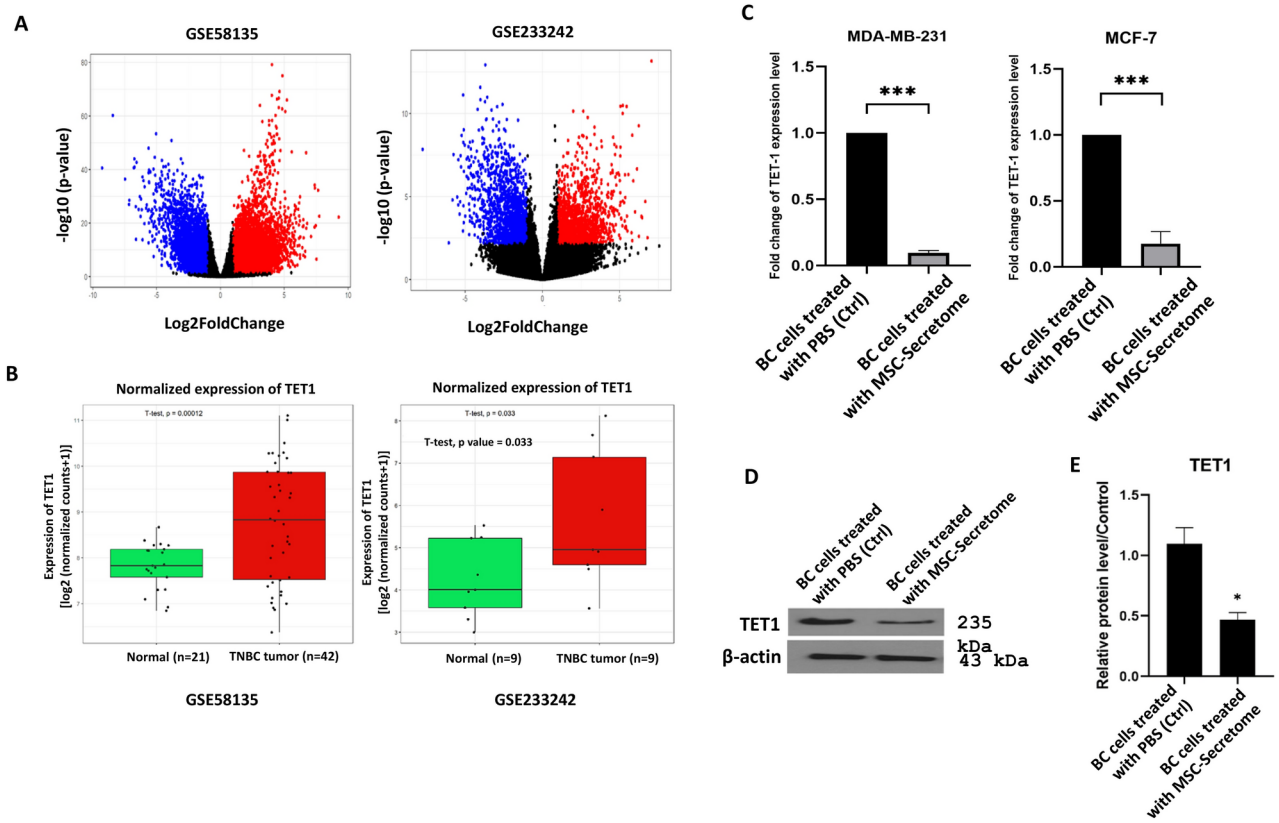

Fig. 3. MSC-derived secretome downregulates TET1 expression in breast cancer cells. **(A, B)** Differential expressed genes (DEGs) and identification of TET1 in TNBC tumors. **A.** Volcano plot showing DEGs from the GSE58135 and GSE233242 datasets, with criteria of P-value < 0.05, adjusted P-value < 0.05, and log fold change (log FC) > 1. Blue dots represent downregulated genes, the red dots indicate upregulated genes, and black dots represent genes with no significant differences in expression. (**B.**) Boxplots displaying normalized TET1 expression levels in TNBC tumors compared to normal tissues. Results indicated upregulation of TET-1 transcript expression in TNBC samples relative to normal tissues across both GSE58135 and GSE233242 datasets. Significance was determined using an unpaired Student's t-test. (**C, D.**) Investigation of TET1 gene expression in BC cells treated with MSC-derived secretome using RT-qPCR and western blot analysis. (**C.**) The mean normalized ratio of TET1 transcript levels was measured by RT-qPCR in MDA-MB-231 and MCF-7 BC cells. Results indicated a significant reduction in TET1 expression in cells treated with MSC-derived secretome compared to control cells. (**D**) Western blot analysis indicated downregulation of TET-1 in MDA-MB-231 cells, 48 h post-treatment with MSC-derived secretome, compared to control cells. β-actin served as a loading control. Western blot images represent at least three independent experiments. Original blots are presented in Supplementary Fig. 1. (**E**) Band densities were quantified using ImageJ software and presented as relative intensities. Data are expressed as the mean ± SD from three independent experiments; $^{*}P < 0.05$, $^{***}P < 0.001$.

the increased sensitivity of siTET1-treated MDA-MB-231 cells to cisplatin over time, suggesting a potential role for TET1 in modulating the cisplatin response.

Discussion

The TME consists of the extracellular matrix (ECM) and signaling molecules that interact with tumor cells. In addition to cancer cells, non-malignant cells such as fibroblasts, endothelial cells, and immune cells, along with the surrounding ECM, collectively influence tumor behavior. Among the various cell sources studied, bone marrow-derived mesenchymal stem cells (BM-MSCs) have garnered significant attention and are prominently featured in this research[25,26]. MSCs have shown considerable promise in treating TNBC by interacting with tumor cells and modulating the tumor microenvironment[8]. Despite significant progress in recent years, the precise mechanisms of MSC interactions with tumor cells are still not fully understood. The tumor-promoting versus tumor-suppressing roles of MSCs have been widely debated over the past decade. While numerous studies suggest that MSCs may enhance tumorigenesis[23,27] other research indicates that MSCs could inhibit tumor progression[28,29]. The tumor-promoting or tumor-suppressing effects of MSCs can be attributed to various factors, including the use of various tumor models, the functional heterogeneity of MSC preparations, and different sources of the MSCs. It is well-established that the paracrine effects of MSCs vary significantly depending on their origin[30,31]. For example, Akimoto et al. (2013) observed distinct interactions between human umbilical cord blood-derived mesenchymal stem cells (UCB-MSCs) and adipose-derived stem cells (ASCs) with

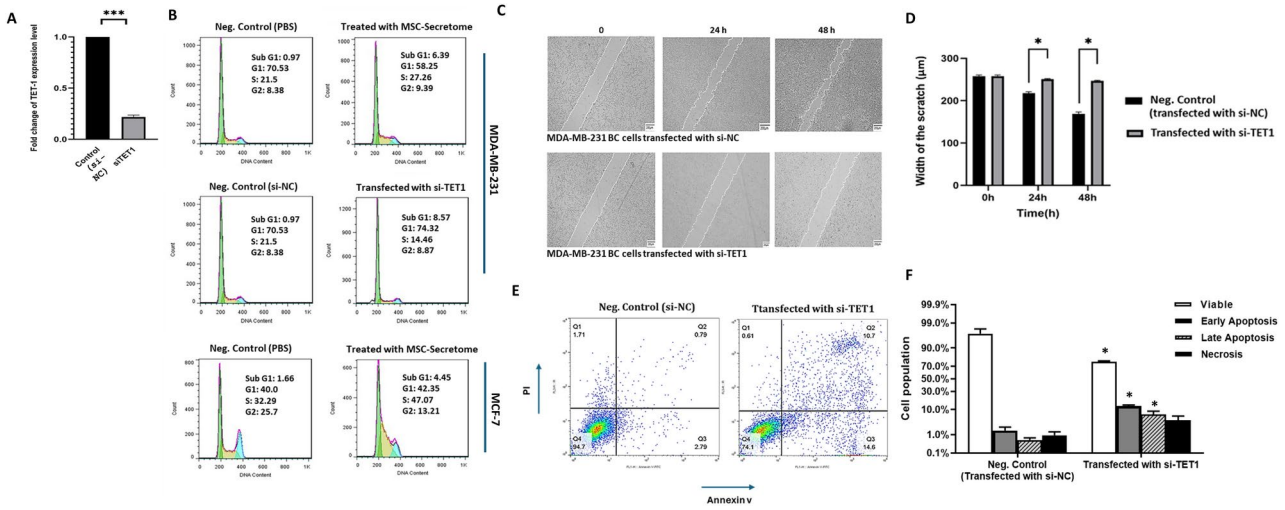

Fig. 4. TET1 downregulation induces cell cycle arrest and triggers apoptosis in breast cancer cells. (**A**) TET1 transcript levels were measured by RT-qPCR in MDA-MB-231 BC cells, showing a significant decrease in TET1 expression in cells transfected with si-TET1 compared to control cells transfected with si-NC. (**B**) Representative flow cytometry histograms of cell cycle distribution in BC cells under different conditions after 48 h of incubation. Results revealed that MSC-derived secretome treatment led to an increased accumulation of cells in the sub G1 phase. Additionally, flow cytometry showed that si-TET1 transfection produced a cell cycle distribution similar to that observed in MSC-secretome-treated MDA-MB-231 cells, indicating a comparable effect on cell cycle arrest. (**C**) Representative images of MDA-MB-231 BC cells transfected with si-TET1 compared to cells transfected with si-NC, at 24 h and 48 h post-scratch wounding. Magnification: 10×. Scale bar = 200 µm. (**D**) Quantitative analysis of cell migration showed that MDA-MB-231 cells transfected with si-TET1 had significantly lower migration potential compared to cells transfected with si-NC. (**E, F**) Representative flow cytometry histograms **(E)** and bar graphs **(F)** illustrating apoptosis in MDA-MB-231 BC cells induced by si-TET1 transfection. Flow cytometry analysis of Annexin V-FITC and PI-stained cells indicated that siRNA targeting TET1 triggers apoptosis compared to the control group. **(F)** shows the mean percentages of viable, early apoptotic, late apoptotic, and necrotic cells following siRNA transfection. Data are expressed as the mean ± SD from three independent experiments; $^{*}P < 0.05$, $^{***}P < 0.001$.

gliomas. In in vitro co-culture studies, UCB-MSCs suppressed the growth of primary glioblastoma multiforme tumor cells and induced apoptosis, while ASCs facilitated cell growth[32].

The secretome released by MSCs represents a novel mechanism underlying their paracrine effects on the tumor microenvironment. This mechanism involves the secretion of various factors and exosomes that collectively influence tumor development and progression[29]. A key question is how to understand the mechanisms by which MSCs function in tumor cell progression. The paracrine effects of MSCs were illustrated by Haynesworth et al.[33], who reported that MSCs synthesize and secrete a variety of growth factors, chemokines, and cytokines that can significantly influence adjacent cells[34]. Recent findings regarding the effects of MSC-secretome on the tumor microenvironment have sparked interest in understanding tumor behavior. Despite important findings in recent years, the exact mechanisms by which MSC secretions exert either stimulatory or inhibitory effects on tumors remain unclear[35]. The secretome derived from MSCs plays an important role in cancer by either promoting or suppressing tumor growth. For instance, several studies have shown that MSCs enhance tumor growth and metastasis in BC[36]. Similarly, Kim et al. demonstrated that conditioned media from human amniotic membrane stromal cells promoted BC proliferation and migration[37]. On the contrary, Matsuzuka et al. investigated the effect of human umbilical cord mesenchymal stem cells (hUCMSCs) on metastatic MDA-MB-231 BC cells, reporting that intravenous injection of hUCMSCs significantly inhibited tumor growth compared to the control group[38]. Additionally, a study by Mirabdollahi et al. found that the secretome derived from Human Wharton's jelly mesenchymal stem cells (hWJMSCs) inhibited the proliferation of MCF-7 BC cells in vitro. Furthermore, intratumoral administration of the hWJMSC secretome led to significant tumor growth inhibition, improved hematological indicators in vivo, and increased long-term survival rates in cancer-bearing mice[39].

Recent evidence has increasingly highlighted the involvement of TET1 in various human diseases, including cancers[40]. However, the precise role of TET1 on cancer development remains a subject of debate. Earlier studies suggest that TET1 functions as a tumor suppressor by binding to the promoters of tumor suppressor genes and reactivating them through active DNA demethylation[41,42]. However, recent studies suggest that TET1 may also contribute to tumor malignancy, with its effects being influenced by its demethylation activity, particularly under low oxygen conditions (hypoxia)[43,44]. Additionally, two separate studies demonstrated that MLL-fusion proteins directly target TET1, significantly increasing its expression in cases of MLL-rearranged leukemia, which leads to widespread elevation of 5-hydroxymethylcytosine levels[45]. The MLL-TET1 fusion protein facilitates the immortalization of myeloid progenitor cells and contributes to leukemia progression[46].

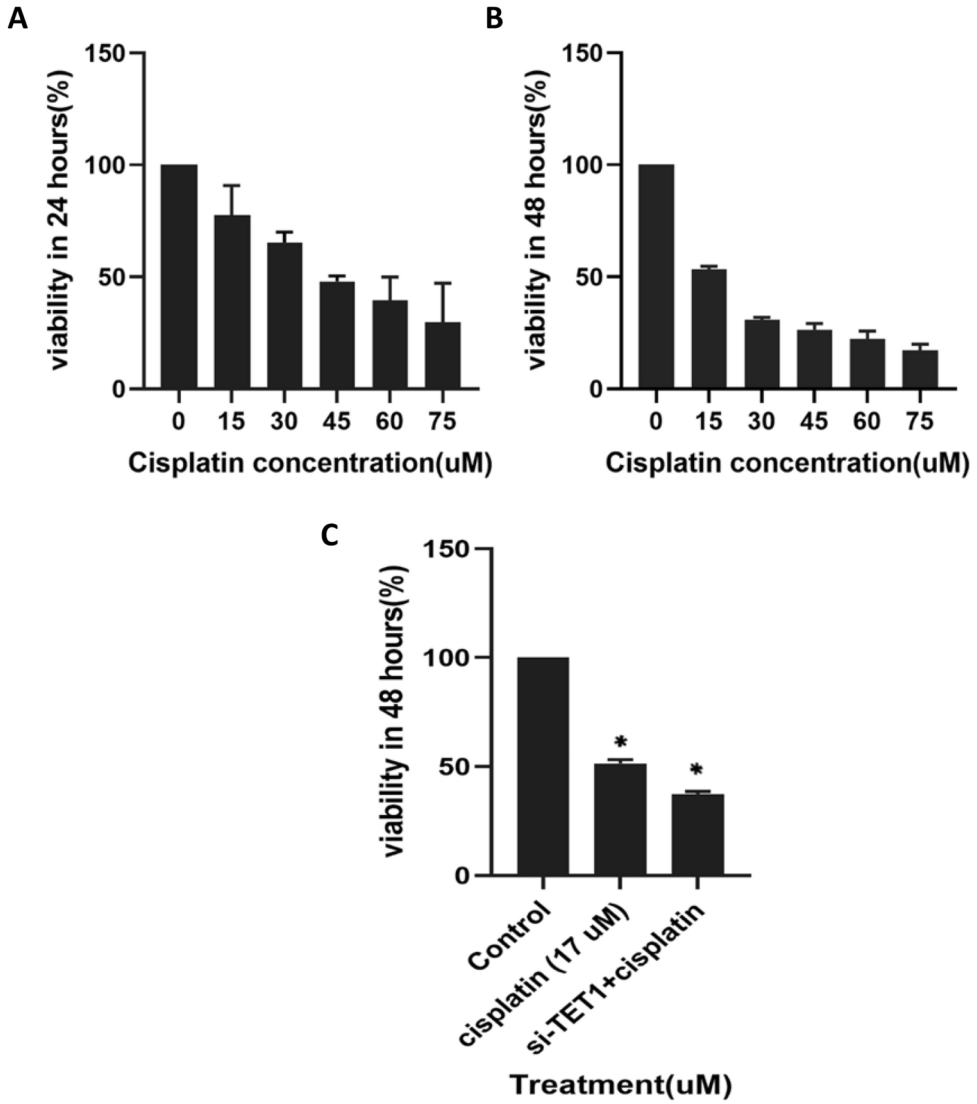

Fig. 5. Targeting TET1 enhances cisplatin sensitivity in breast cancer cells. **(A, B)** MDA-MB-231 BC cell viability was measured as a function of cisplatin concentration to determine the IC50 at 24 and 48 h post-treatment. **(C)** MTT assay results showed that TET1 suppression via si-TET1 transfection increased the sensitivity of MDA-MB-231 cells to cisplatin, with a more pronounced decline in cell viability at the IC50 concentration observed at 48 h. These findings suggest a potential role of TET1 in mediating cisplatin resistance in breast cancer. Data are expressed as the mean ± SD from three independent experiments; $^{*}P < 0.05$.

In this study, it was observed that inhibiting TET1 expression increased sensitivity to cisplatin. Growing evidence supports the role of TET1 in platinum resistance across various cancers. A similar study demonstrated that cisplatin resistance is driven by TET1 expression, with vimentin identified as a specific target of TET1's function in ovarian cancer[47]. Likewise, Kang et al. reported that reducing TET1 expression via siRNA enhanced the responsiveness of colorectal cancer cells to treatment with cisplatin and 5-fluorouracil[48].

Our study found that downregulating TET1 directly affected the migration of MDA-MB-231 cells, suggesting that TET1 plays a role in promoting this migratory ability. TET1 has also been reported to enhance the migration of DLD1 colon cancer cells through a mechanism involving the downregulation of E-cadherin, mediated by H3K27me3[49]. Another finding in colon cancer showed that suppressing TET1 counteracted the excessive gene expression induced by tumor hypoxia and reduced the migration ability of tumor cells[50]. Under hypoxic conditions, upregulation of TET1 expression has been shown to enhance the migration and proliferation of trophoblast cells through the HIF1α signaling pathway[51]. However, our study found that reducing TET1 expression via MSC-secretome treatment inhibits the migration and proliferation of cancer cells. This suggests that TET1 may play a similar but context-dependent role in promoting cellular capabilities across different environments and cell types.

Achieving reproducibility in studies involving MSC-conditioned medium (MSC-CM) is essential, given that MSC secretion profiles can vary significantly depending on cell source, isolation methods, and culture conditions. Consistent sourcing of MSCs—whether derived from bone marrow, adipose tissue, or other

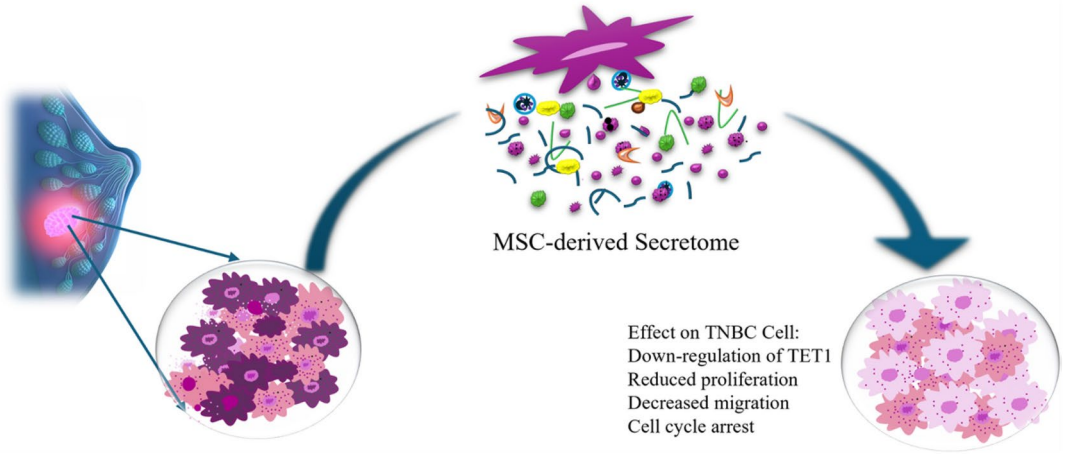

Fig. 6. Schematic model illustrating MSC-mediated modulation of breast cancer cell progression via secretome. The MSC-derived secretome inhibits proliferation and migration of TNBC cells, downregulates TET1 expression, and reduces protein markers associated with breast cancer progression.

origins—is necessary, as variations in origin impact their secreted factors, including cytokines and exosomes. Standardizing MSC isolation and preparation methods, alongside comprehensive profiling of MSC-CM using omics technologies, can help ensure the consistency of bioactive molecules in these preparations. Rigorous preclinical validation using standardized animal models, such as patient-derived xenografts (PDX) or genetically engineered mice, is also critical for assessing the translational potential of MSC-CM. For clinical translation, Good Manufacturing Practice (GMP)-compliant production is essential to ensure quality, safety, and efficacy. Additionally, 3D co-culture models that more accurately replicate the tumor microenvironment, coupled with detailed gene expression monitoring, can further validate the functional consistency of MSC-CM, facilitating the reliable translation of these findings into clinical applications.

Overall, our study provides critical insights into the effects of MSC-secretome on BC cells. We demonstrated that MSC-secretome treatment is associated with reduced migration and proliferation of BC cells, underscoring its potential therapeutic impact (Fig. 6). Additionally, downregulating TET1 expression in TNBC offers a more detailed molecular explanation of how the MSC-secretome influences TNBC progression. These findings suggest that TET1 could be a valuable biomarker for predicting cisplatin treatment efficacy and BC metastasis, and may help stratify TNBC patients for targeted therapies.

Materials and methods

Primary cell culture

Human bone marrow-derived MSCs were obtained from bone marrow aspirates of five healthy individuals undergoing marrow harvesting for allogeneic transplantation, as previously described[52]. The study was approved by the Institutional Ethics Board of Tarbiat Modares University, with ethical approval code IR.MODARES.REC.1401.235, and written informed consent was obtained from the participants. The study was conducted in accordance with the Declaration of Helsinki. MSC quality and performance are influenced by intrinsic donor characteristics, such as age[53]. Since the proliferation and differentiation capacities of MSCs tend to decline with age, cells were obtained from young donors aged 25–35. Briefly, mononuclear cells were isolated by density gradient centrifugation with Ficoll-Paque. After centrifugation at $400 \times g$ for 30 min, the mononuclear cell layer was collected and washed twice with PBS. Cells were then seeded in tissue culture flasks at a density of 1×10^6 cells/mL in Dulbecco's Modified Eagle Medium (DMEM) supplemented with 10% fetal bovine serum (FBS) and 1% antibiotics (100 U/mL penicillin and 100 µg/mL streptomycin) (All from Gibco BRL, Rockville, MD, USA). Cultures were maintained at 37 °C in a humidified incubator with 5% CO2, with medium changes every 3–4 days to remove non-adherent cells. When cultures reached approximately 80–90% confluency, adherent cells were detached with trypsin–EDTA and either passaged for further expansion or used for downstream experiments. To collect the secretome, MSCs were serum-starved upon reaching over 80% confluency. After 48 h, the conditioned media (CM) were collected, pooled, and centrifuged at $300 \times g$ for 10 min, followed by a second centrifugation at $10{,}000 \times g$ for 30 min to eliminate residual cells and cellular debris. The total protein concentration of the MSC secretome was measured using the BCA assay and found to be 653 µg/mL. For comparison, the protein concentration of the control media was about 7 µg/mL. For BC treatment, the concentrated MSC-derived secretome was diluted with control complete medium containing 10% FBS to achieve a final concentration of 50% secretome (1:2 dilution).

Cell lines

Human breast carcinoma cell lines MDA-MB-231 and MCF-7 were obtained from the Pasteur Institute of Iran. Both cell lines were maintained in DMEM supplemented with 10% heat-inactivated FBS and 1% antibiotics (100 U/ml penicillin, and 100 µg/ml streptomycin; all from Gibco, USA) at 37 °C in a humidified incubator with 5% CO2.

Mesenchymal stem cell characterization

The morphology of BM-MSCs was monitored using an inverted microscope (CETI, Belgium). Cell surface marker expression was analyzed by flow cytometry, assessing positive markers such as CD73, CD90, CD105, as well as the negative selection markers CD34 and CD11b[54]. To assess the differentiation capability of BM-MSCs, cells were cultured in osteogenic conditions with 2 mM β-glycerophosphate, 100 µM L-ascorbic acid 2-phosphate, and 10 nM dexamethasone (All from Sigma). Following induction, cultures were stained with Alizarin Red to visualize mineralization. For adipogenic induction, the culture medium was supplemented with 500 nM isobutylmethylxanthine, 60 µM indomethacin, 500 nM hydrocortisone, 10 µg/ml insulin (Sigma), 100 nM L-ascorbic acid phosphate. After 10 days, the cells were stained with Oil Red O, and lipid droplets were visualized using optical microscopy.

Identification of differentially expressed genes (DEGs)

The bulk RNA sequencing data for TNBC tumors and normal tissues were obtained from GSE233242, which includes 9 pairs of TNBC and matched normal breast tissues from the same patients. Additionally, data from GSE58135 included 42 primary TNBC tumors and 21 adjacent uninvolved breast tissue samples. Both datasets are available in the GEO database (https://www.ncbi.nlm.nih.gov/). After selecting the desired datasets, the quality of the reads was assessed using Fast QC, and reads were trimmed with Trimmomatic[55]. Next, the trimmed sequencing data were mapped to the human genome (hg38) with HISAT2[56], and read counts were generated with HTSeq[57]. Differentially expressed genes (DEG) were identified using DESeq2[58]. We applied filters to the DEG results with threshold of p-value < 0.05, adjusted p-value < 0.05, and log fold change ≥ 1 for upregulated genes and log fold change ≤ − 1 for downregulated genes.

siRNA transfection

Two independent siRNAs targeting TET1 (50 nM) and a negative control siRNA (si-NC; GenePharma) were introduced into MDA-MB-231 cells (2×10^4) using Lipofectamine 2000 (Thermo Fisher Scientific, USA). The sequences of siRNAs were as follows: TET1 si-RNA1 sense: 5′-GAAGCGAAGAAACCCUUUATT-3′; antisense: 5′-UAAAGGGUUUCUUCGCUUCTT-3′; TET1 si-RNA2 sense: 5′-GCGAAAGGUACAAAUUAAUTT-3′; antisense: 5′-AUUAAUUUGUACCUUUCGCTT-3′, and si-NC sense: 5′-UUCUCCGAACGUGUCACGUTT-3′; antisense: 5′-ACGUGACACGUUCGGAGAATT-3′.

RNA extraction and quantitative real-time PCR

Total RNA was isolated from BC cells using TRIzol (Invitrogen, USA). Subsequently, complementary DNA (cDNA) synthesis was performed using the RevertAid First-Strand cDNA Synthesis Kit (Takara, Japan). Reverse transcription quantitative real-time PCR (RT-qPCR) was conducted using the ABI Step One Sequence Detection System (Applied Biosystems, USA) with SYBR Premix Ex Taq™ II (TAKARA, Japan). Human Beta-2 microglobulin (β2m) was utilized as internal control to normalize gene expression data. The primer sequences utilized in the RT-qPCR assay were as follows: TET1**:** Forward: 5′-CATCAGTCAAGACTTTAAGCCCT-3′, Reverse: 5′-CGGGTGGTTTAGGTTCTGTTT-3′ and ß2M: Forward: 5′-CTCCGTGGCCTTAGCTGTG-3′, Reverse: 5′-TTGGAGTACGCTGGATAGCC-3′.

Cell proliferation assay

MDA-MB-231 and MCF-7 cells (2×10^5 cells/well each) were seeded into 6-well plates and treated with 1000 µl of MSC-derived secretome or vehicle control, using appropriate culture media, and incubated overnight. Viable cells were counted in triplicate at 0-, 24-, 48-, and 72-h post-incubation using trypan blue exclusion. Briefly, viable cell counting was performed with a Neubauer hemocytometer. After harvesting, the cell suspension was mixed with 0.4% Trypan Blue to distinguish live (unstained) from dead cells (blue-stained). The mixture was loaded onto the hemocytometer, and viable cells were counted under a light microscope. Cell proliferation was calculated as the number of viable cells per mL.

Scratch wound healing assay

To assess the migration capability of MDA-MB-231 and MCF-7 cells in vitro, the scratch method was employed. A sterile 100 µL pipette tip was used to create a vertical scratch in the cell monolayer. Subsequently, BC cells were treated with MSC-derived secretome or negative control (culture media without FBS) for 0, 24, and 48 h. A similar assay was conducted with MDA-MB-231 cells transfected with 40 µL siTET1 or its corresponding negative control. Wound healing was monitored, and the extent of scratch closure was then measured and analyzed with Image J (V1.52).

MTT assay

Cell viability was assessed using the MTT assay, following the manufacturer's instructions (Sigma-Aldrich, USA). Cells were seeded into 96-well plates at a concentration of 10,000 cells per well and allowed to adhere overnight. Subsequently, the cells were exposed to varying concentrations of Cisplatin (0, 15, 30, 45, 60, 75 µM) or a control for 48 h. After the treatment period, the growth medium was discarded, and the cells were subjected to a 3 h incubation at 37 °C with 0.5 mg/mL MTT solution in a serum-free medium. The resulting MTT solution was aspirated, and 100 µL of dimethyl sulfoxide (DMSO) was added to each well. The absorbance of the formazan solution was then measured at 570 nm using a microplate reader (BioTek, USA). To account for any non-specific signals, background absorbance at 690 nm was subtracted. The procedures for the MTT assay, aimed at assessing the emergence of drug resistance in cells subjected to siTET1 treatment, mirrored the previous methods. However, a modification was made to determine the cisplatin IC50 dose prior to application, followed by the administration of siTET1 treatment to the cells.

Cell cycle analysis
To determine the cell cycle phase of BC cells by flow cytometry, MDA-MB-231 and MCF-7 cells were treated with 2 mL MSC-derived secretome. Additionally, a separate group of MDA-MB-231 cells was transfected with si-TET1, as described above. After a 48-h treatment with Triton X-100 and RNase A, the BC cells were collected and stained with propidium iodide (PI, Sigma). Cellular DNA content was then analyzed using a flow cytometer, and the distribution of BC cells across different cell cycle phases was calculated using Flowjo (V10).

Apoptosis analysis
The Annexin-V-FITC staining kit (Sigma-Aldrich, USA) was used to quantify the number of cells undergoing apoptosis. Cells were seeded onto six-well plates (0.3×10^6 cells/well) and incubated for 24 h at 37 °C. MDA-MB-231 cells was then harvested by trypsinization, centrifuged at $1500 \times g$ for 6 min, and washed with ice-cold PBS. The resulting cell pellet was resuspended in 100 µl of 1X Annexin-binding buffer along with 100 µg/ml solution of propidium iodide (PI) and incubated in the dark for 10–15 min. The stained cells were promptly analyzed using flow cytometry (BD FACSCanto II flow Cytometer, USA). Early apoptotic cells were identified by Annexin V-FITC staining, while cells in later stages of apoptosis exhibited positive staining for both Annexin V-FITC and PI.

Western blotting
MDA-MB-231 BC cells (2×10^6) were lysed in 500 µL of lysis buffer (50 mM Tris–HCl at pH 8.0, 150 mM NaCl, 2 mM EDTA and 0.1% NP-40) containing a protease inhibitor cocktail (Roche). After incubation on ice for 30 min, lysates were centrifuged at $12{,}000 \times g$ for 10 min at 4 °C to remove cellular debris. Total protein concentration was quantified using the BCA protein assay kit, following the manufacturer's instructions. For gel loading, 20 µg of protein from each sample was mixed with loading buffer and denatured at 95 °C for 5 min. Equal protein amounts were loaded onto 10% SDS–polyacrylamide gel electrophoresis (SDS-PAGE) and separated by electrophoresis. The protein bands separated by SDS-PAGE were transferred onto polyvinylidene difluoride (PVDF) membranes. The 5% skimmed milk was prepared in TBST (Tris-Buffered Saline with Tween 20) buffer and used as a blocking agent. The antibodies were also diluted in TBS-T buffer containing skimmed milk. The membranes were incubated with the primary antibody for 12 h at 4 °C, followed by a 1-h incubation with a horseradish peroxidase (HRP)-conjugated secondary antibody at room temperature. Enhanced chemiluminescence was then performed using an ECL kit (Amersham, UK). The membranes were developed using the GE Amersham Imager chemiluminescence imaging system. The primary antibodies used were: c-Myc (9E10) (sc-40, 1:1000; Santa Cruz Biotechnology), Cyclin D1 (A-12) (sc-8396, 1:1000; Santa Cruz Biotechnology), TET1 (4F4) (sc-293186, 1:1000; Santa Cruz Biotechnology), E-cadherin (67A4) (sc-21791, 1:1000; Santa Cruz Biotechnology), and N-cadherin (E-AB-70061, 1:1000; Elabscience Biotechnology Inc.). The secondary antibodies used were: m-IgGκ BP-HRP (sc-516102, 1:2000; Santa Cruz Biotechnology) and mouse anti-rabbit IgG-HRP (sc-2357, 1:2000; Santa Cruz Biotechnology). β-Actin (2A3) (sc-517582, 1:200; Santa Cruz Biotechnology) was used as the loading control.

Statistical analysis
Experiments were conducted independently at least three times. Statistical analyses were performed using FlowJo software version 7.6.1 (FlowJo LLC, Ashland, OR) and GraphPad Prism 9 (GraphPad Software, Inc, La Jolla, CA, USA). An unpaired t-test was utilized for statistical comparisons, with significance defined as $P < 0.05$.

Data availability
The data supporting the findings of this study are available from the corresponding author upon reasonable request.

Received: 31 July 2024; Accepted: 19 February 2025
Published online: 24 February 2025

References
1. Bareche, Y. et al. Unravelling triple-negative breast cancer molecular heterogeneity using an integrative multiomic analysis. *Ann. Oncol. Off. J. Eur. Soc. Med. Oncol.* **29**(4), 895–902. https://doi.org/10.1093/annonc/mdy024 (2018).
2. Derakhshan, F. & Reis-Filho, J. S. Pathogenesis of triple-negative breast cancer. *Annu. Rev. Pathol.* **17**, 181–204. https://doi.org/10.1146/annurev-pathol-042420-093238 (2022).
3. Savas, P. et al. Clinical relevance of host immunity in breast cancer: From TILs to the clinic. *Nat. Rev. Clin. Oncol.* **13**(4), 228–241. https://doi.org/10.1038/nrclinonc.2015.215 (2016).
4. Deepak, K. G. K. et al. Tumor microenvironment: Challenges and opportunities in targeting metastasis of triple negative breast cancer. *Pharmacol. Res.* **153**, 104683. https://doi.org/10.1016/j.phrs.2020.104683 (2020).
5. Yu, T. & Di, G. Role of tumor microenvironment in triple-negative breast cancer and its prognostic significance. *Chin. J. Cancer Res.* **29**(3), 237–252. https://doi.org/10.21147/j.issn.1000-9604.2017.03.10 (2017).
6. Stevens, K. N., Vachon, C. M. & Couch, F. J. Genetic susceptibility to triple-negative breast cancer. *Cancer Res.* **73**(7), 2025–2030. https://doi.org/10.1158/0008-5472.CAN-12-1699 (2013).
7. Sturtz, L. A. et al. Gene expression differences in adipose tissue associated with breast tumorigenesis. *Adipocyte.* **3**(2), 107–114. https://doi.org/10.4161/adip.28250 (2014).
8. Wu, Y., Shum, H. C. E., Wu, K. & Vadgama, J. From interaction to intervention: How mesenchymal stem cells affect and target triple-negative breast cancer. *Biomedicines.* https://doi.org/10.3390/biomedicines11041182 (2023).
9. Väänänen, H. K. Mesenchymal stem cells. *Ann. Med.* **37**(7), 469–479. https://doi.org/10.1080/07853890500371957 (2005).
10. Eltoukhy, H. S., Sinha, G., Moore, C. A., Gergues, M. & Rameshwar, P. Secretome within the bone marrow microenvironment: A basis for mesenchymal stem cell treatment and role in cancer dormancy. *Biochimie.* **155**, 92–103. https://doi.org/10.1016/j.biochi.2018.05.018 (2018).

11. Silva, M., Monteiro, G. A., Fialho, A. M., Bernardes, N. & da Silva, C. L. Conditioned medium from Azurin-expressing human mesenchymal stromal cells demonstrates antitumor activity against breast and lung cancer cell lines. *Front. Cell Dev. Biol.* **8**, 471. https://doi.org/10.3389/fcell.2020.00471 (2020).
12. Ahn, S. Y. The role of MSCs in the tumor microenvironment and tumor progression. *Anticancer Res.* **40**(6), 3039–3047. https://doi.org/10.21873/anticanres.14284 (2020).
13. Slama, Y. et al. The dual role of mesenchymal stem cells in cancer pathophysiology: Pro-tumorigenic effects versus therapeutic potential. *Int. J. Mol. Sci.* https://doi.org/10.3390/ijms241713511 (2023).
14. Ayuzawa, R. et al. Naïve human umbilical cord matrix derived stem cells significantly attenuate growth of human breast cancer cells in vitro and in vivo. *Cancer Lett.* **280**(1), 31–37 (2009).
15. Zohora, F. T., Aliyu, M. & Saboor-Yaraghi, A. A. Secretome-based acellular therapy of bone marrow-derived mesenchymal stem cells in degenerative and immunological disorders: A narrative review. *Heliyon.* **9**(7), e18120. https://doi.org/10.1016/j.heliyon.2023.e18120 (2023).
16. Tomasetti, C., Marchionni, L., Nowak, M. A., Parmigiani, G. & Vogelstein, B. Only three driver gene mutations are required for the development of lung and colorectal cancers. *Proc. Natl. Acad. Sci. USA.* **112**(1), 118–123. https://doi.org/10.1073/pnas.1421839112 (2015).
17. Vizoso, F. J., Eiro, N., Cid, S., Schneider, J. & Perez-Fernandez, R. Mesenchymal stem cell secretome: toward cell-free therapeutic strategies in regenerative medicine. *Int. J. Mol. Sci.* https://doi.org/10.3390/ijms18091852 (2017).
18. Schultz, N. Comprehensive molecular portraits of human breast tumours. *Nature.* **490**(7418), 61–70. https://doi.org/10.1038/nature11412 (2012).
19. Stefansson, O. A. et al. A DNA methylation-based definition of biologically distinct breast cancer subtypes. *Mol. Oncol.* **9**(3), 555–568. https://doi.org/10.1016/j.molonc.2014.10.012 (2015).
20. Ghazimoradi, M. H., Pakravan, K., Khalafizadeh, A. & Babashah, S. TET1 regulates stem cell properties and cell cycle of cancer stem cells in triple-negative breast cancer via DNA demethylation. *Biochem. Pharmacol.* **219**, 115913. https://doi.org/10.1016/j.bcp.2023.115913 (2024).
21. Ito, S. et al. Tet proteins can convert 5-methylcytosine to 5-formylcytosine and 5-carboxylcytosine. *Science.* **333**(6047), 1300–1303. https://doi.org/10.1126/science.1210597 (2011).
22. Liu, W., Wu, G., Xiong, F. & Chen, Y. Advances in the DNA methylation hydroxylase TET1. *Biomark Res.* **9**(1), 76. https://doi.org/10.1186/s40364-021-00331-7 (2021).
23. Almouh, M. et al. Exosomes released by oxidative stress-induced mesenchymal stem cells promote murine mammary tumor progression through activating the STAT3 signaling pathway. *Mol. Cell Biochem.* https://doi.org/10.1007/s11010-024-04934-0 (2024).
24. Good, C. R. et al. TET1-mediated hypomethylation activates oncogenic signaling in triple-negative breast cancer. *Cancer Res.* **78**(15), 4126–4137. https://doi.org/10.1158/0008-5472.CAN-17-2082 (2018).
25. Sun, Z., Wang, S. & Zhao, R. C. The roles of mesenchymal stem cells in tumor inflammatory microenvironment. *J. Hematol. Oncol.* **7**, 14. https://doi.org/10.1186/1756-8722-7-14 (2014).
26. Zhou, X. et al. Mesenchymal stem cell-derived extracellular vesicles promote the in vitro proliferation and migration of breast cancer cells through the activation of the ERK pathway. *Int. J. Oncol.* **54**(5), 1843–1852. https://doi.org/10.3892/ijo.2019.4747 (2019).
27. Galiè, M. et al. Mesenchymal stem cells share molecular signature with mesenchymal tumor cells and favor early tumor growth in syngeneic mice. *Oncogene.* **27**(18), 2542–2551. https://doi.org/10.1038/sj.onc.1210920 (2008).
28. Khakoo, A. Y. et al. Human mesenchymal stem cells exert potent antitumorigenic effects in a model of Kaposi's sarcoma. *J. Exp. Med.* **203**(5), 1235–1247. https://doi.org/10.1084/jem.20051921 (2006).
29. Pakravan, K. et al. MicroRNA-100 shuttled by mesenchymal stem cell-derived exosomes suppresses in vitro angiogenesis through modulating the mTOR/HIF-1α/VEGF signaling axis in breast cancer cells. *Cell Oncol.* **40**(5), 457–470. https://doi.org/10.1007/s13402-017-0335-7 (2017).
30. Pires, A. O. et al. Unveiling the differences of secretome of human bone marrow mesenchymal stem cells, adipose tissue-derived stem cells, and human umbilical cord perivascular cells: A proteomic analysis. *Stem Cells Dev.* **25**(14), 1073–1083. https://doi.org/10.1089/scd.2016.0048 (2016).
31. Gomes, E. D., de Castro, J. V., Costa, B. M. & Salgado, A. J. The impact of mesenchymal stem cells and their secretome as a treatment for gliomas. *Biochimie.* **1**(155), 59–66. https://doi.org/10.1016/j.biochi.2018.07.008 (2018).
32. Akimoto, K. et al. Umbilical cord blood-derived mesenchymal stem cells inhibit, but adipose tissue-derived mesenchymal stem cells promote, glioblastoma multiforme proliferation. *Stem Cells Dev.* **22**(9), 1370–1386. https://doi.org/10.1089/scd.2012.0486 (2013).
33. Haynesworth, S. E., Baber, M. A. & Caplan, A. I. Cytokine expression by human marrow-derived mesenchymal progenitor cells in vitro: Effects of dexamethasone and IL-1 alpha. *J. Cell Physiol.* **166**(3), 585–592 (1996).
34. Lai, R. C., Yeo, R. W. Y. & Lim, S. K. Mesenchymal stem cell exosomes. *Semin Cell Dev Biol.* **40**, 82–88. https://doi.org/10.1016/j.semcdb.2015.03.001 (2015).
35. Ritter, A. et al. Adipose tissue-derived mesenchymal stromal/stem cells, obesity and the tumor microenvironment of breast cancer. *Cancers.* https://doi.org/10.3390/cancers14163908 (2022).
36. Yu, P. F. et al. TNFα-activated mesenchymal stromal cells promote breast cancer metastasis by recruiting CXCR2(+) neutrophils. *Oncogene.* **36**(4), 482–490. https://doi.org/10.1038/onc.2016.217 (2017).
37. Kim, S. H. et al. Human amniotic membrane-derived stromal cells (hAMSC) interact depending on breast cancer cell type through secreted molecules. *Tissue Cell.* **47**(1), 10–16. https://doi.org/10.1016/j.tice.2014.10.003 (2015).
38. Matsuzuka, T. et al. Human umbilical cord matrix-derived stem cells expressing interferon-beta gene significantly attenuate bronchioloalveolar carcinoma xenografts in SCID mice. *Lung Cancer.* **70**(1), 28–36. https://doi.org/10.1016/j.lungcan.2010.01.003 (2010).
39. Mirabdollahi, M., Sadeghi-Aliabadi, H. & Haghjooy, J. S. Human Wharton's jelly mesenchymal stem cells-derived secretome could inhibit breast cancer growth in vitro and in vivo. *Iran J. Basic Med. Sci.* **23**(7), 945–953. https://doi.org/10.22038/ijbms.2020.42477.10020 (2020).
40. Li, L. et al. Epigenetic inactivation of the CpG demethylase TET1 as a DNA methylation feedback loop in human cancers. *Sci. Rep.* **6**, 26591. https://doi.org/10.1038/srep26591 (2016).
41. Choudhury, S. R., Cui, Y., Lubecka, K., Stefanska, B. & Irudayaraj, J. CRISPR-dCas9 mediated TET1 targeting for selective DNA demethylation at BRCA1 promoter. *Oncotarget.* **7**(29), 46545–46556. https://doi.org/10.18632/oncotarget.10234 (2016).
42. Pei, Y. F. et al. TET1 inhibits gastric cancer growth and metastasis by PTEN demethylation and re-expression. *Oncotarget.* **7**(21), 31322–31335. https://doi.org/10.18632/oncotarget.8900 (2016).
43. Yang, Q. et al. Hypoxia switches TET1 from being tumor-suppressive to oncogenic. *Oncogene.* **42**(20), 1634–1648. https://doi.org/10.1038/s41388-023-02659-w (2023).
44. Tsai, Y. P. et al. TET1 regulates hypoxia-induced epithelial-mesenchymal transition by acting as a co-activator. *Genome Biol.* **15**(12), 513. https://doi.org/10.1186/s13059-014-0513-0 (2014).
45. Huang, H. et al. TET1 plays an essential oncogenic role in MLL-rearranged leukemia. *Proc. Natl. Acad. Sci. USA.* **110**(29), 11994–11999. https://doi.org/10.1073/pnas.1310656110 (2013).

46. Kim, H. S. et al. MLL-TET1 fusion protein promotes immortalization of myeloid progenitor cells and leukemia development. *Haematologica.* **102**(11), e434–e437. https://doi.org/10.3324/haematol.2017.169789 (2017).
47. Han, X. et al. TET1 promotes cisplatin-resistance via demethylating the vimentin promoter in ovarian cancer. *Cell Biol. Int.* **41**(4), 405–414. https://doi.org/10.1002/cbin.10734 (2017).
48. Kang, K. A. et al. Epigenetic modification of Nrf2 in 5-fluorouracil-resistant colon cancer cells: Involvement of TET-dependent DNA demethylation. *Cell Death Dis.* **5**(4), e1183. https://doi.org/10.1038/cddis.2014.149 (2014).
49. Zhou, Z. et al. Loss of TET1 facilitates DLD1 colon cancer cell migration via H3K27me3-mediated down-regulation of E-cadherin. *J. Cell Physiol.* **233**(2), 1359–1369. https://doi.org/10.1002/jcp.26012 (2018).
50. Ma, L. et al. Tet methylcytosine dioxygenase 1 promotes hypoxic gene induction and cell migration in colon cancer. *J. Cell Physiol.* **234**(5), 6286–6297. https://doi.org/10.1002/jcp.27359 (2019).
51. Zhu, J. et al. Hypoxia-induced TET1 facilitates trophoblast cell migration and invasion through HIF1α signaling pathway. *Sci. Rep.* **7**(1), 8077. https://doi.org/10.1038/s41598-017-07560-7 (2017).
52. Potian, J. A., Aviv, H., Ponzio, N. M., Harrison, J. S. & Rameshwar, P. Veto-like activity of mesenchymal stem cells: Functional discrimination between cellular responses to alloantigens and recall antigens. *J. Immunol.* **171**(7), 3426–3434. https://doi.org/10.4049/jimmunol.171.7.3426 (2003).
53. Maged, G., Abdelsamed, M. A., Wang, H. & Lotfy, A. The potency of mesenchymal stem/stromal cells: Does donor sex matter?. *Stem Cell Res. Ther.* **15**(1), 112. https://doi.org/10.1186/s13287-024-03722-3 (2024).
54. Mirabdollahi, M., Haghjooyjavanmard, S. & Sadeghi-Aliabadi, H. An anticancer effect of umbilical cord-derived mesenchymal stem cell secretome on the breast cancer cell line. *Cell Tissue Bank.* **20**(3), 423–434. https://doi.org/10.1007/s10561-019-09781-8 (2019).
55. Bolger, A. M., Lohse, M. & Usadel, B. Trimmomatic: A flexible trimmer for Illumina sequence data. *Bioinformatics.* **30**(15), 2114–2120. https://doi.org/10.1093/bioinformatics/btu170 (2014).
56. Kim, D., Langmead, B. & Salzberg, S. L. HISAT: A fast spliced aligner with low memory requirements. *Nat. Methods.* **12**(4), 357–360. https://doi.org/10.1038/nmeth.3317 (2015).
57. Anders, S., Pyl, P. T. & Huber, W. HTSeq–a Python framework to work with high-throughput sequencing data. *Bioinformatics.* **31**(2), 166–169. https://doi.org/10.1093/bioinformatics/btu638 (2015).
58. Love, M. I., Huber, W. & Anders, S. Moderated estimation of fold change and dispersion for RNA-seq data with DESeq2. *Genome Biol.* **15**(12), 550. https://doi.org/10.1186/s13059-014-0550-8 (2014).

Acknowledgements

The authors are grateful to the members of the Department of Molecular Genetics at Tarbiat Modares University for their excellent support and contributions.

Author contributions

R.M., K.J., and M.S. performed all the experiments. M.G. and S.G. conducted investigations and interpreted data. M.G. and M.J. contributed study materials and conducted the bioinformatics analyses. R.M. and K.J. drafted the original version of the manuscript. N.H. and S.B. edited and reviewed the manuscript. S.B. conceived and supervised the study and provided administrative support. All authors reviewed and approved the final manuscript.

Funding

This work was funded by the Iran National Science Foundation (INSF) under project No. 4036036 and supported by Tarbiat Modares University.

Declarations

Competing interests

The authors declare no competing interests.

Additional information

Supplementary Information The online version contains supplementary material available at https://doi.org/10.1038/s41598-025-91314-3.

Correspondence and requests for materials should be addressed to S.B.